

Fig S1 Patient enrollment flow chart

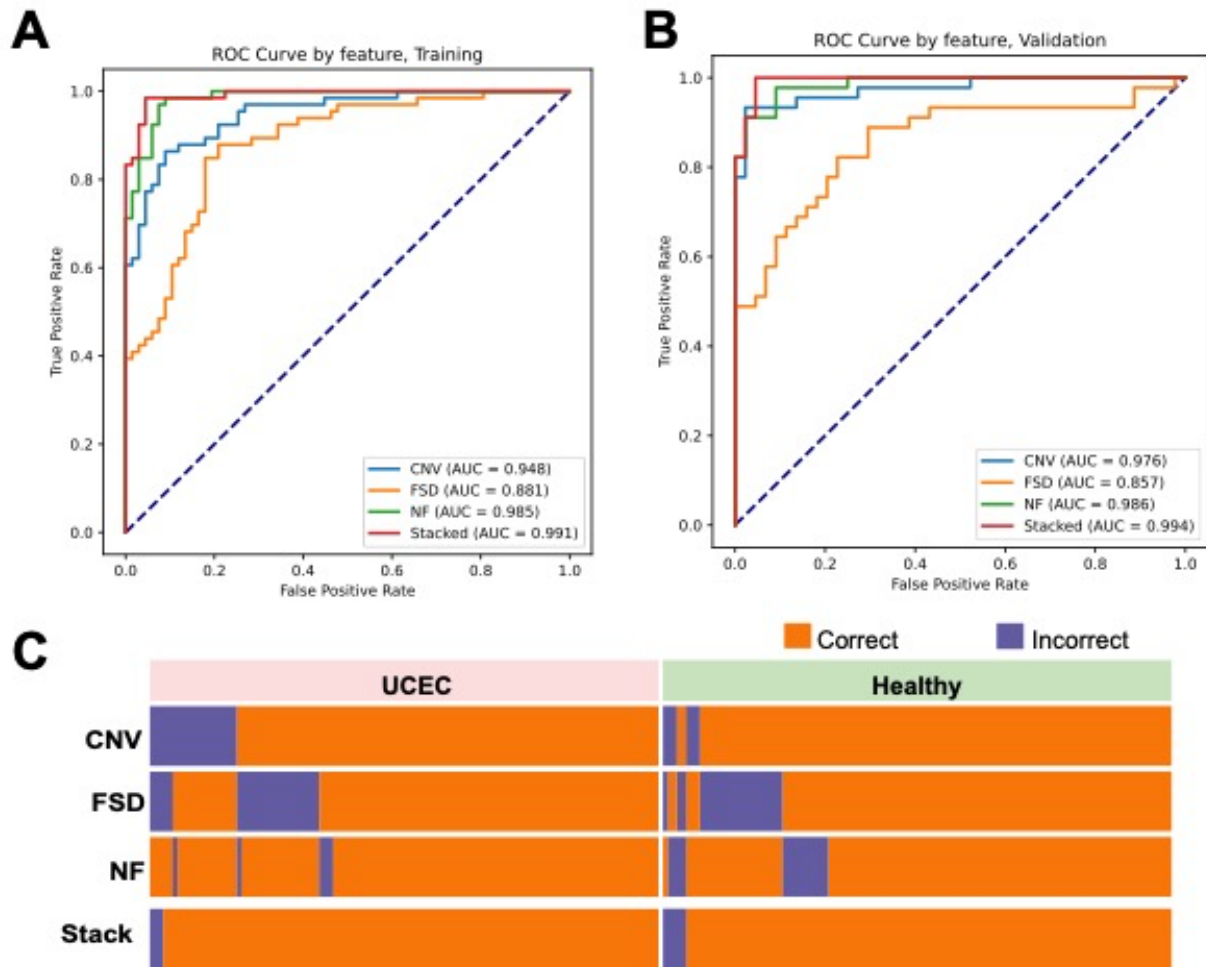


Fig S2 A-B Training ROC curve of base models constructed upon individual features (CNV, FSD and NF) and their ensemble stack model for training (A) and validation (B) cohort. **C Prediction agreement with true labels for each case under three single-feature model and the ensemble stacked model**

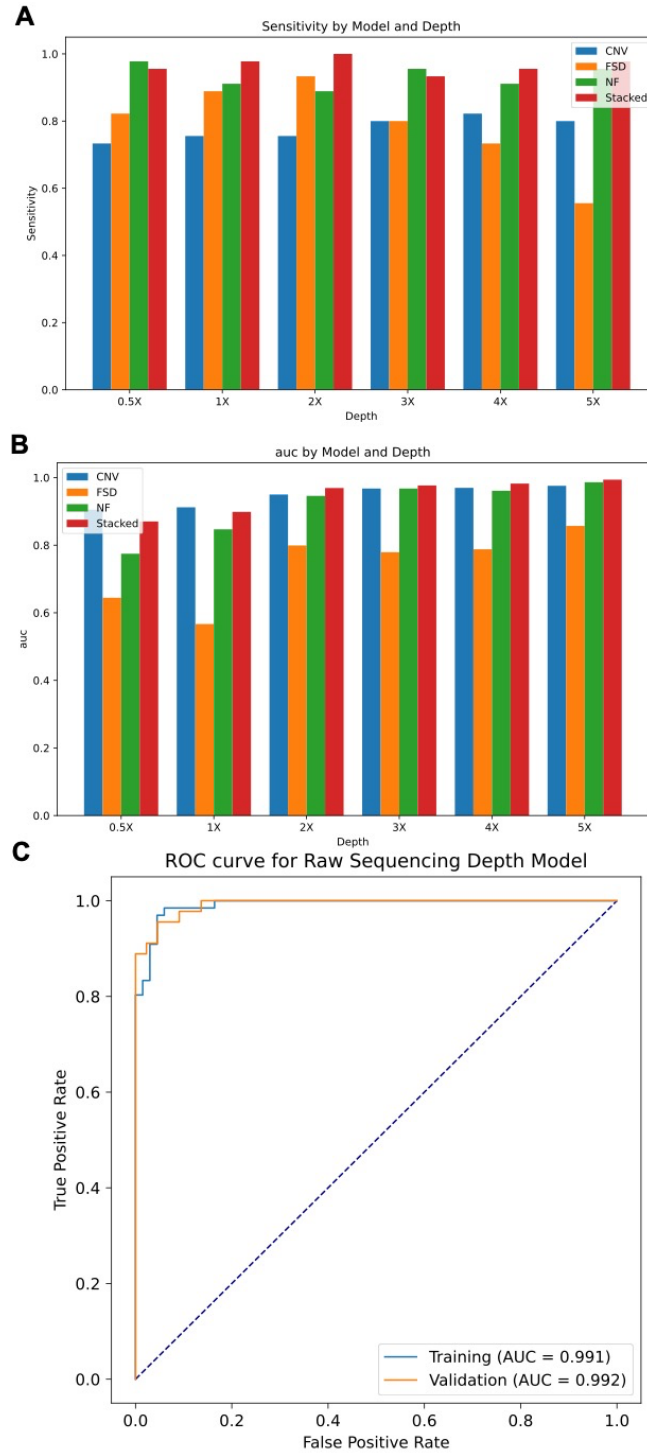


Fig S3 Sensitivity (A) and AUC (B) of the model on validation cohort with lower sequencing coverage depth. C ROC curve of model constructed using raw sequencing depth data.

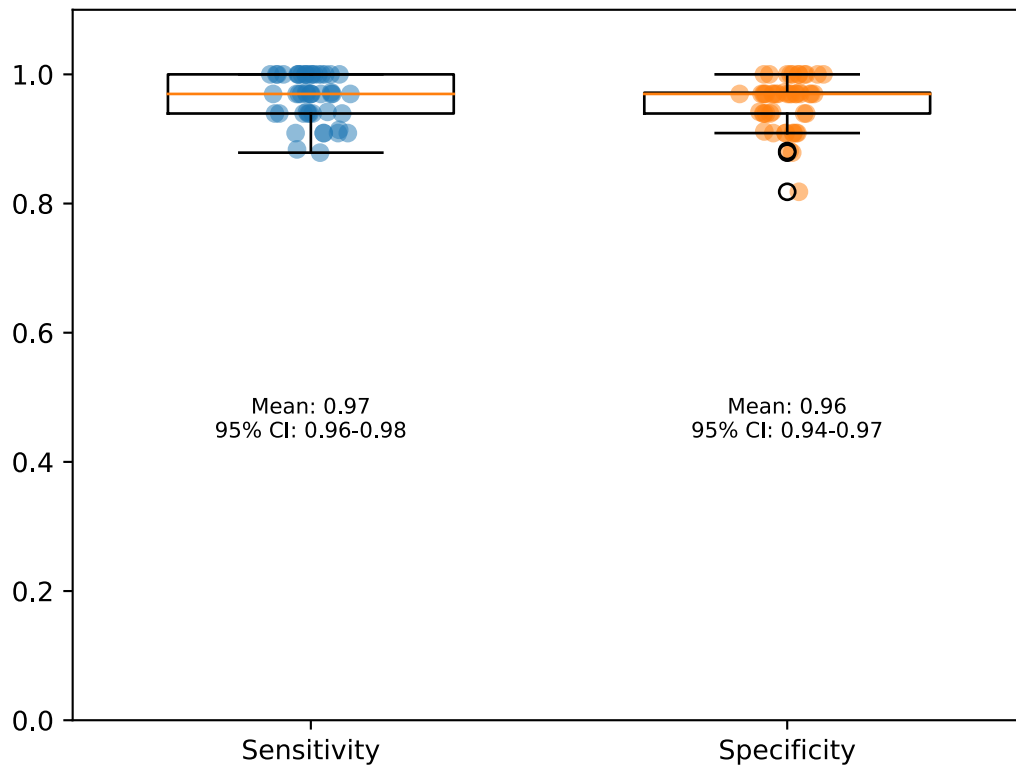


Fig S4 Model Performance Evaluation through Repeated Random Partitioning of the Cohort

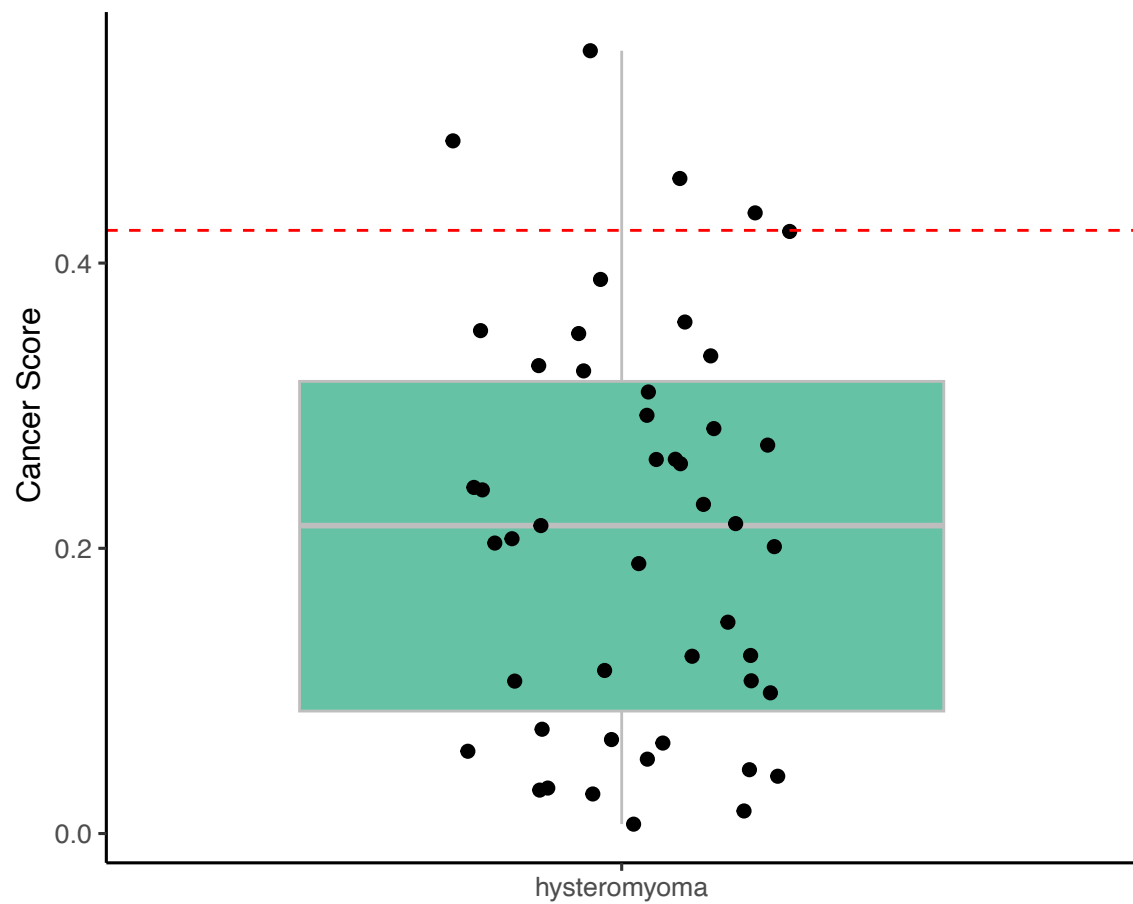
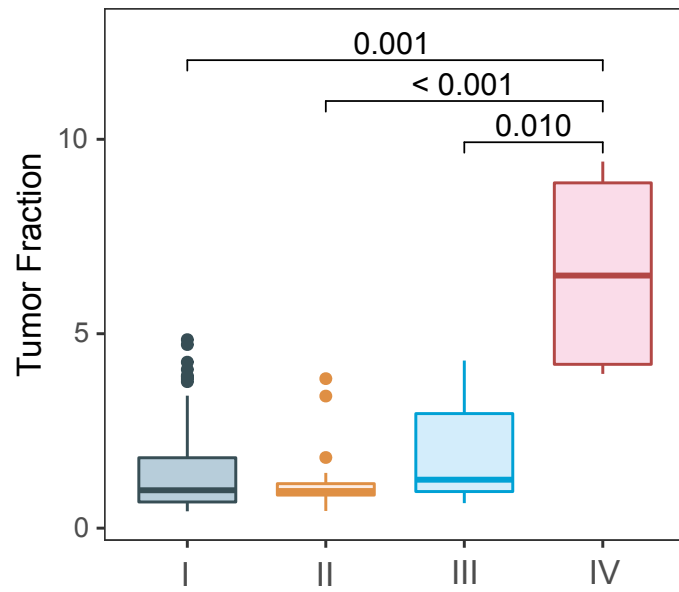


Fig S5 Cancer scores of 47 hysteromyoma patients

A



B

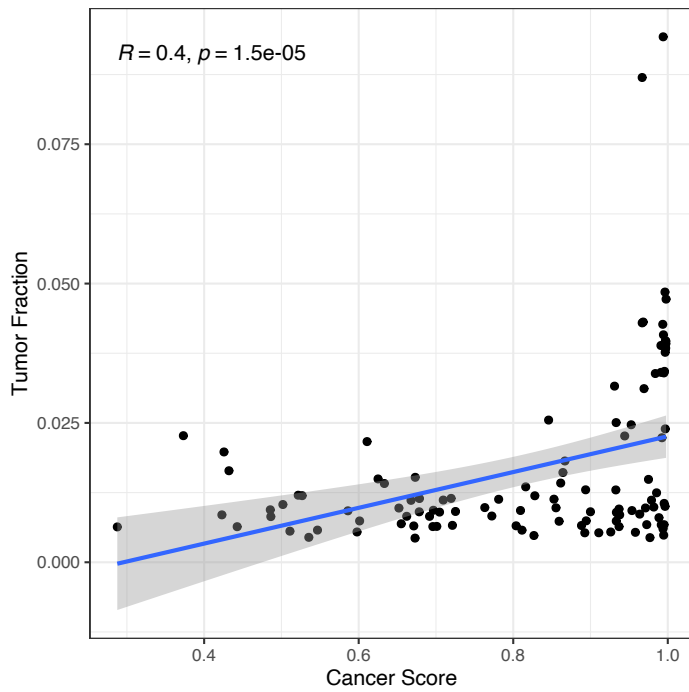


Fig S6 **A** The correlation of tumor fraction and stage. **B** Scatter plot illustrating the positive correlation between the cancer scores and the tumor fraction.

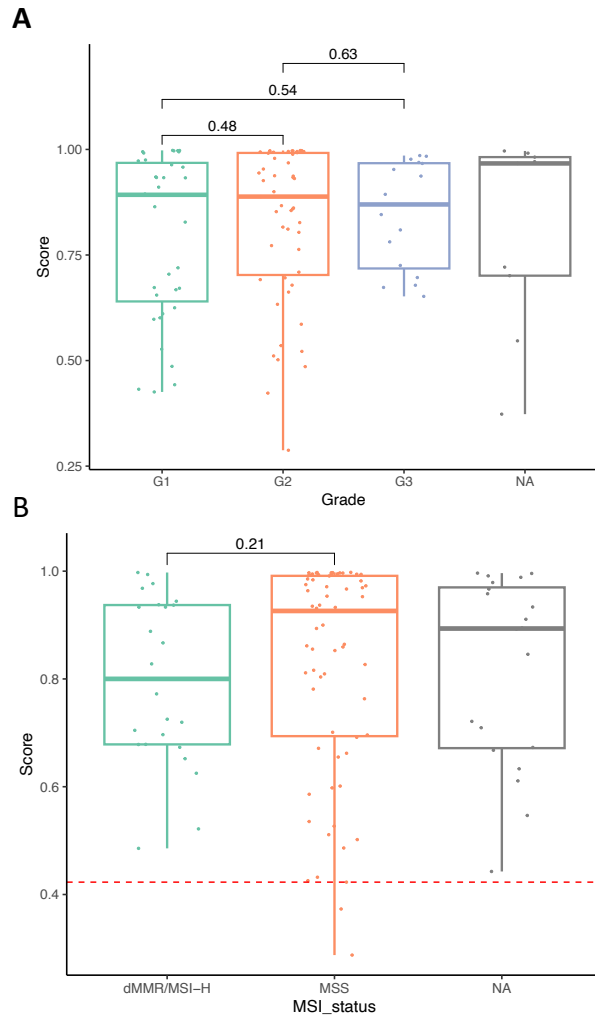


Fig S7. Boxplot comparing cancer scores in samples with different grade (A) and MSI status (B)

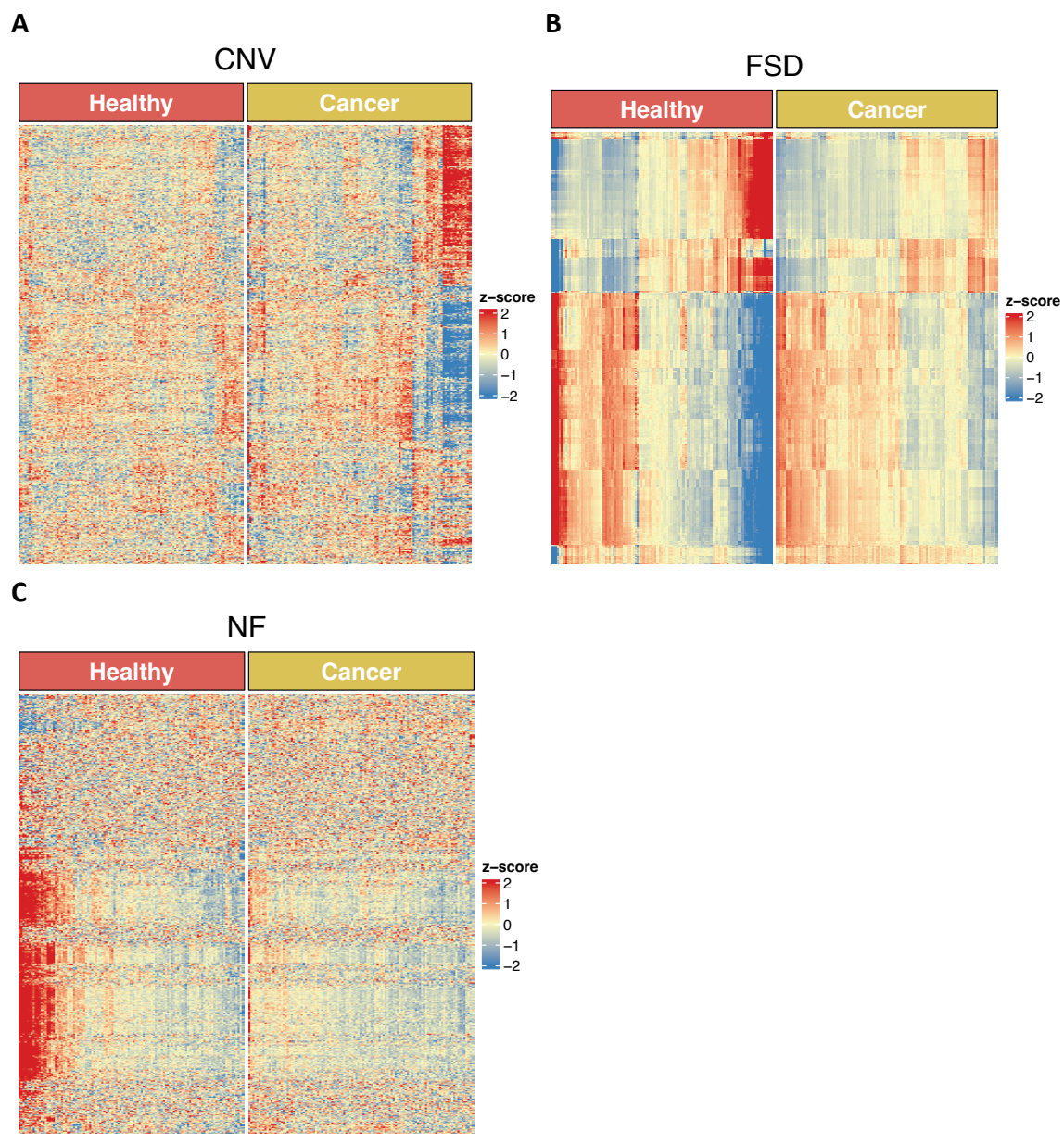


Fig S8. Heatmap showed CNV(A), FSD(B) and NF(C) features between UCEC patients and healthy control.

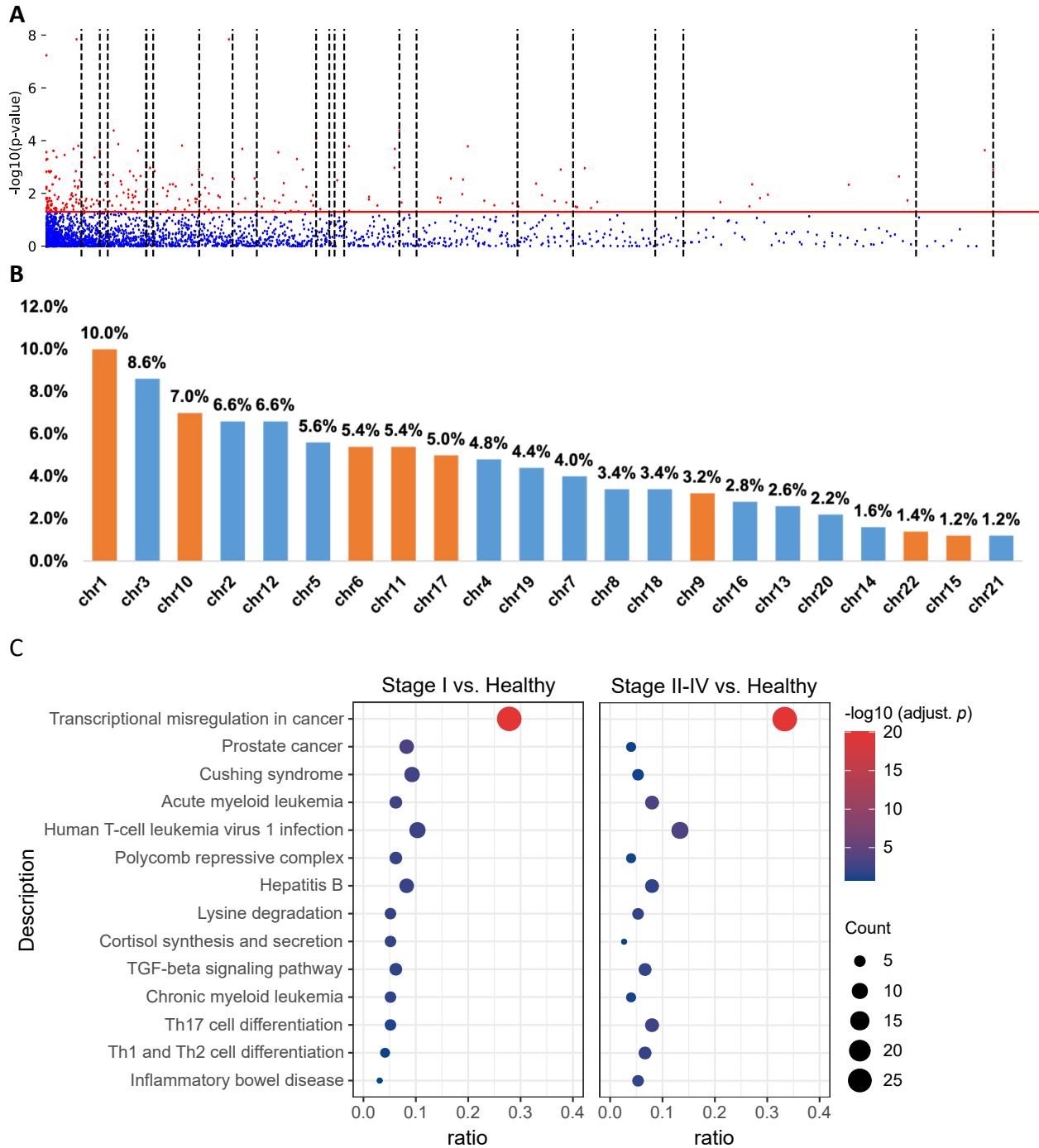


Fig S9. A CNV feature difference between UCEC patients and healthy controls. Red dots indicated a significant adjusted p-value. **B** The mutation frequency of each chromosome in TCGA-UCEC database. **C** KEGG pathway enrichment analysis of genes corresponding to NF features that displayed distinct characteristics in early stage and late stage UCEC patients versus healthy controls.

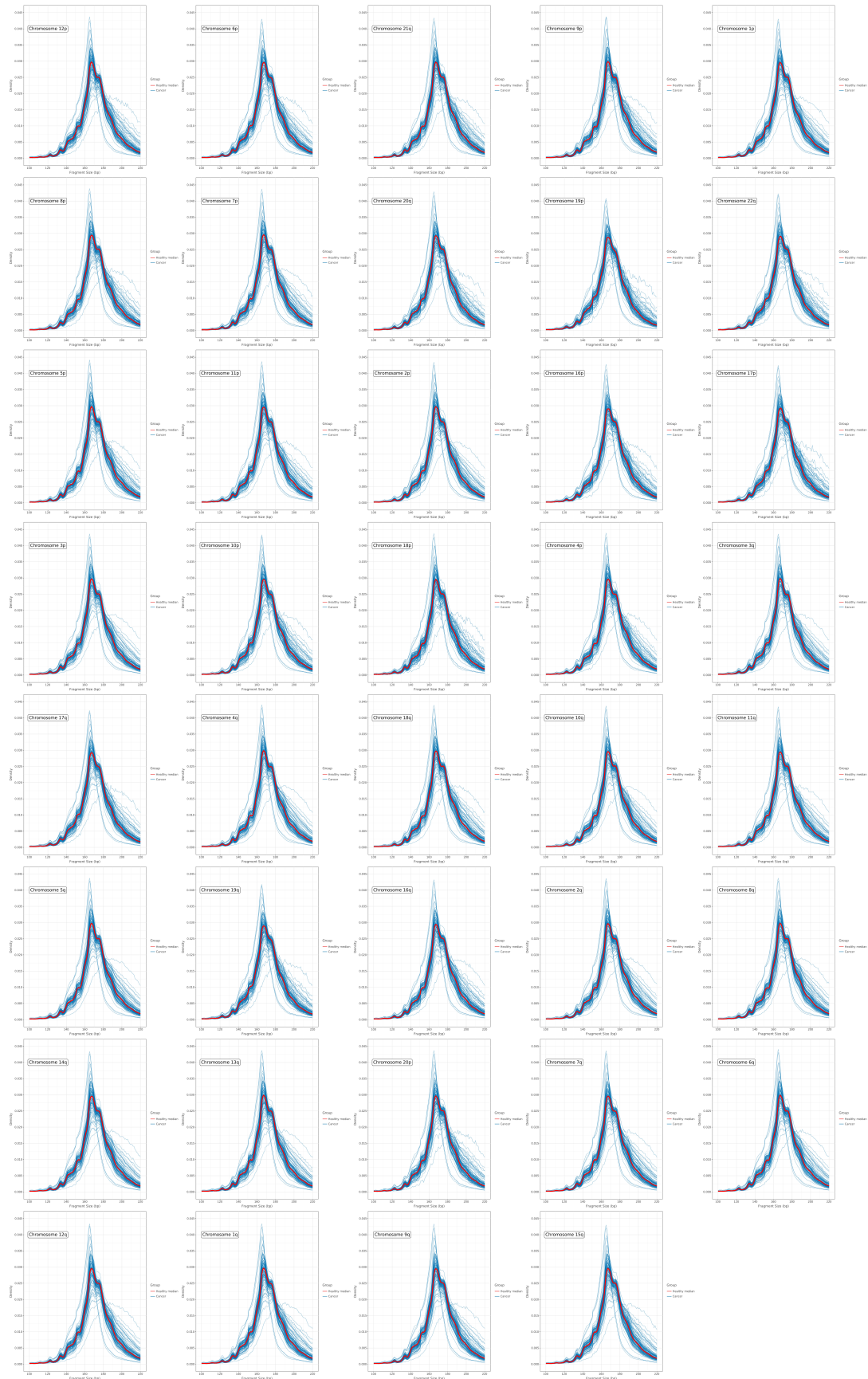


Fig S10. Fragment length distribution between the UCEC and healthy donors across each chromosome arms.

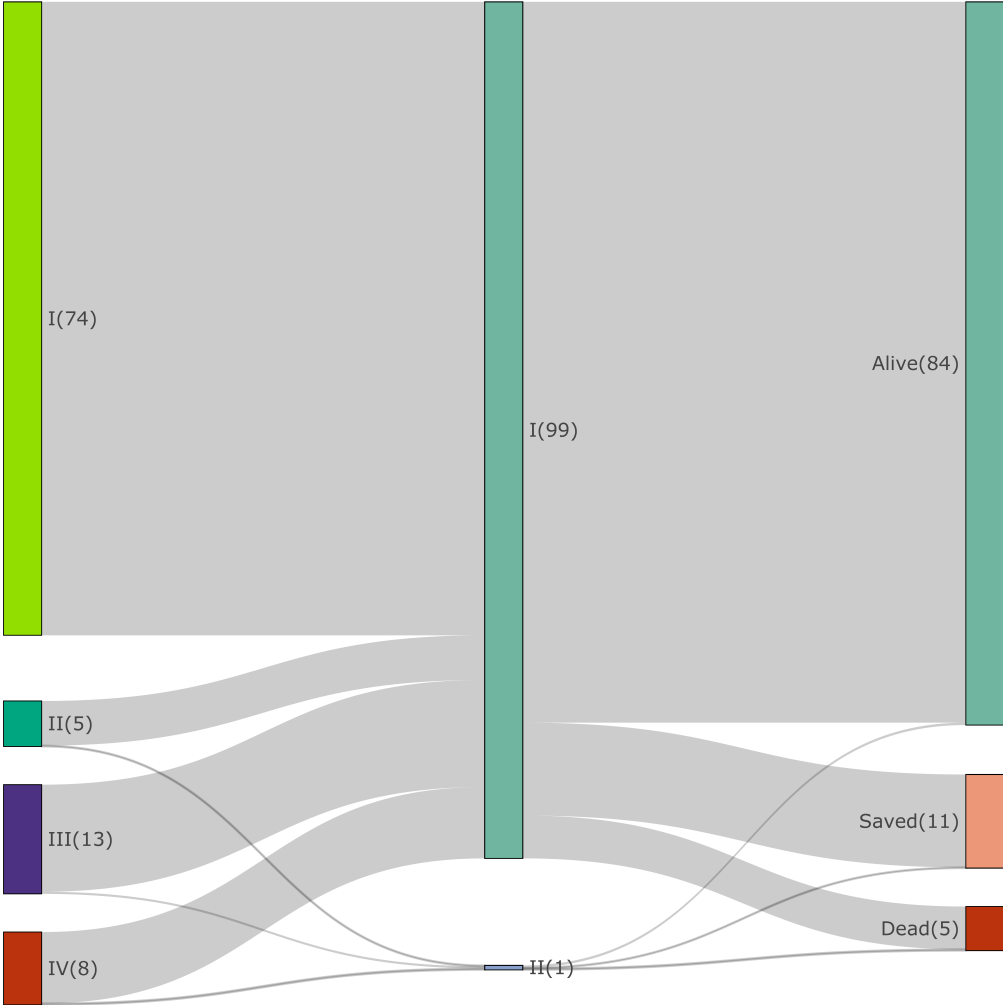


Fig S11 Stage shift analysis by the classifier in a real-world setting among the Chinese population. Sankey plot demonstrating the proportion of patients at each cancer stage at diagnosis, with and without the interception of the classifier, along with potential outcomes in real world.